Role of Solvent on Protein-Matrix Coupling in MbCO Embedded in Water-Saccharide Systems: A Fourier Transform Infrared Spectroscopy Study

Sergio Giuffrida, Grazia Cottone, and Lorenzo Cordone
Dipartimento di Scienze Fisiche ed Astronomiche, Università di Palermo and CNISM, I-90123 Palermo, Italy

ABSTRACT Embedding protein in sugar systems of low water content enables one to investigate the protein dynamic-structure function in matrixes whose rigidity is modulated by varying the content of residual water. Accordingly, studying the dynamics and structure thermal evolution of a protein in sugar systems of different hydration constitutes a tool for disentangling solvent rigidity from temperature effects. Furthermore, studies performed using different sugars may give information on how the detailed composition of the surrounding solvent affects the internal protein dynamics and structural evolution. In this work, we compare Fourier transform infrared spectroscopy measurements (300–20 K) on MbCO embedded in trehalose, sucrose, maltose, raffinose, and glucose matrixes of different water content. At all the water contents investigated, the protein-solvent coupling was tighter in trehalose than in the other sugars, thus suggesting a molecular basis for the trehalose peculiarity. These results are in line with the observation that protein-matrix phase separation takes place in lysozyme-lactose, whereas it is absent in lysozyme-trehalose systems; indeed, these behaviors may respectively be due to the lack or presence of suitable water-mediated hydrogen-bond networks, which match the protein surface to the surroundings. The above processes might be at the basis of pattern recognition in crowded living systems; indeed, hydration shells structural and dynamic matching is first needed for successful come together of interacting biomolecules.

INTRODUCTION

Trehalose (Fig. 1 *a*) is a nonreducing disaccharide of glucose present in large amounts in organisms that can survive adverse environmental conditions such as extreme drought and high temperatures (1–5). Furthermore, it has been observed that isolated structures, such as enzymes or liposomes, are preserved against stressing conditions when embedded in trehalose matrixes (6–8). An analogous protective effect is also accomplished by other saccharides, although trehalose is the most effective in terms of structural and functional recovery (9).

Several studies have been performed on sugar-water biomolecule systems by experimental (10–35) and simulative techniques (36–42). This notwithstanding, the molecular mechanisms at the basis of the trehalose peculiarity are still a matter of study. The main hypotheses proposed are:

i. The water replacement hypothesis, according to which stabilization occurs via the formation of hydrogen bonds (HBs) between the sugar and the biostructure (43);
ii. The water-entrapment hypothesis, according to which, in the dry state, trehalose rather than directly binding to proteins traps the residual water at the biomolecule-sugar interface by glass formation (44);
iii. The high viscosity hypothesis, according to which viscosity effects cause motion inhibition (45) and hindering of processes leading to loss of structure and denaturation. In this respect, Green and Angell (46) suggested the peculiarity of trehalose to be related to its rather high glass transition temperature with respect to other glass-forming sugars.

In the recent past, experimental (10–16,18,22–30,34,35) and molecular dynamics (MD) (36) studies on carboxy-myoglobin (MbCO) embedded in trehalose-water matrixes of low water content showed that in such systems the internal protein dynamics is sizably reduced; furthermore, it was shown (26,28–34,37) that the content of residual water modulates the dynamics and structural evolution of both external matrix and protein. Such information evidenced how embedding protein in water-sugar systems, in which the amount of residual water is varied, could be a useful tool to investigate the temperature dependence of the protein dynamic-structure function relationship as a function of the solvent rigidity, thus enabling one to disentangle rigidity from temperature effects. In particular, a series of Fourier transform infrared spectroscopy (FTIR) measurements were performed on samples of MbCO embedded in nonliquid water-trehalose matrixes in which the thermal evolution of the stretching band of the bound CO and the thermal evolution of the water-association band were contemporarily followed (29,30,34).

As well known, the stretching band of the bound CO molecule in MbCO is commonly split into three subbands attributed to three different conformational substates of the protein (taxonomic or A substates) corresponding to three different environments experienced by the CO molecule within the heme pocket (47,48). The relative intensity, width,

Submitted January 24, 2006, and accepted for publication May 8, 2006.

Address reprint requests to Lorenzo Cordone, E-mail: cordone@fisica.unipa.it.

0006-3495/06/08/968/13 $2.00

doi: 10.1529/biophysj.106.081927

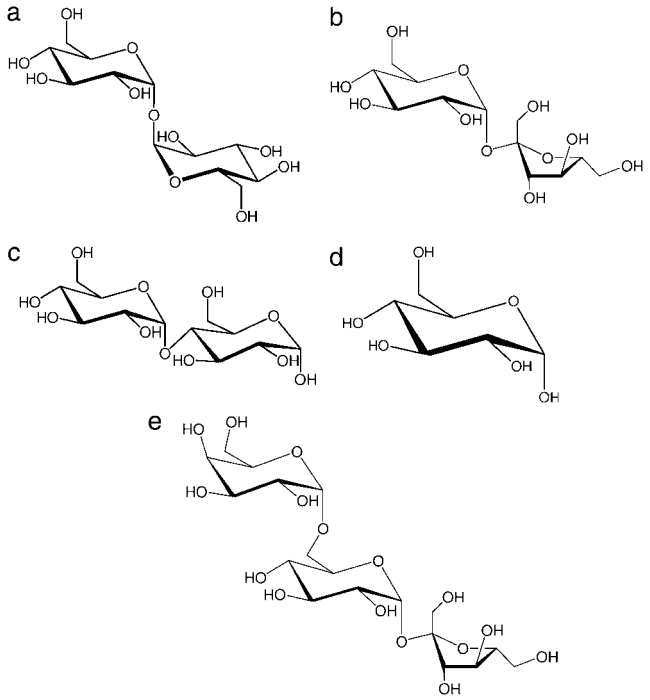

FIGURE 1 Structure of trehalose (*a*), saccharose (*b*), maltose (*c*), glucose (*d*), and raffinose (*e*).

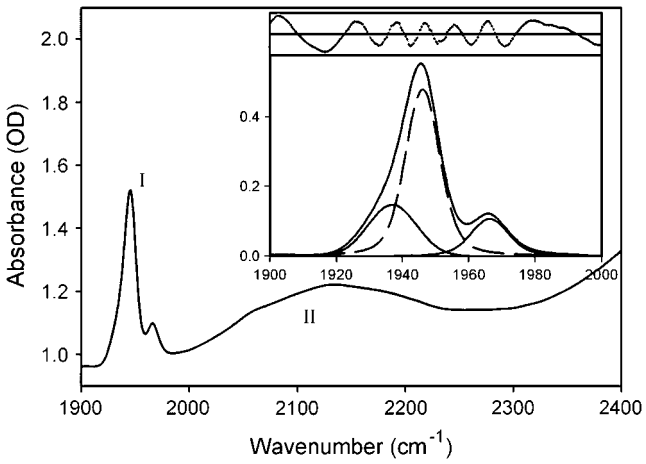

FIGURE 2 CO stretching band (*I*, 1900–2000 cm^{-1}) and association band of water (*II*, 2000–2400 cm^{-1}) in 3_T sample at 300 K. Inset shows the fitting of the CO band in terms of three taxonomic A substates (47). Residuals are also shown in the inset on expanded scale (×100). A Gaussian extrapolation took into account the queue of the association band in the range 1900–2000 cm^{-1}. The fitting of the water-association band was performed in terms of Gaussian and/or Voigtian components, which were dependent on the sample humidity. A Gaussian extrapolation took into account the queue of the adjacent higher frequency bands (>2400 cm^{-1}). Fittings gave the areas under the absorption profiles that were used for normalization of the raw spectra after subtraction of the extrapolation.

and peak position of the three subbands depend on several external parameters such as temperature, pH, and pressure (47–53); accordingly, the thermal evolution of the band shape gives information on the thermal interconversion among taxonomic and lower hierarchy substates.

On the high frequency side of the CO stretching band appears the so-called water-association band (see Fig.2), which, in pure water, is attributed to a combination of the bending mode of water molecules with intermolecular water-water vibrations (54). Furthermore, it has been suggested that the coupling of water-bending modes with intermolecular vibrations involving nonwater H-bonding groups may also contribute to the band (29,30,34). This makes the band useful to get information on the structural behavior of water in the sample under conditions of low water content in which bulk water does not fully cover the signal.

The thermal evolution (300–20 K) of both the above bands was put on a quantitative ground by using the spectra distance (SD) of the normalized bands, defined as (29)

$$\mathrm{SD} = \{\sum[A(\nu,T) - A(\nu,T = 20\mathrm{K})]^2 \Delta\nu\}^{1/2}, \qquad (1)$$

where $A(\nu)$ is the normalized absorbance at the frequency ν and $\Delta\nu$ is the frequency resolution; such quantity represents the deviation of the normalized spectrum at temperature T from the spectrum at 20 K. Accordingly, the temperature dependence of the SD relative to the CO stretching band (SD_{CO}) was assumed to reflect the overall thermally induced changes of the protein structure, as experienced by the bound CO molecule. Considering that such structural changes imply protein internal motions, SD_{CO} also conveys information on the internal protein dynamics.

In aqueous glycerol solutions of MbCO, the second moment (M_2) of the A_0 and A_1 taxonomic substates was found to be constant for T lower than the solvent transition temperature (T_c), and sharply increasing upon heating for $T > T_c$ (55). Such behavior was attributed to the interaction of the CO vibration with large amplitude, low frequency motions of the heme environment, which are only populated in liquid environment, i.e., for $T > T_c$. In this respect, we note that all the samples we studied never behave as liquid. In particular, dry and very dry samples are solid glasses in which the above low frequency motions cannot be populated, whereas humid samples behave, at room temperature, as plasticized and amorphous (see sample preparation); this makes low frequency motions barely populated even at room temperature. Accordingly, the M_2 values of A_1 and A_0 must have a much lower increase than in liquid water glycerol solutions (55); this is confirmed when fitting the CO stretching band (data not shown). The above arguments indicate that the coupling with low frequency motions of the heme environment has, if any, negligible effect on the high temperature values of SD_{CO}.

As mentioned above, the water-association band is useful to get information on the structural behavior of the water in the sample under conditions of low water content. Using the same arguments as for SD_{CO}, the thermal behavior of the SD relative to the water-association band (SD_{WATER}) was assumed to convey information on the thermally induced

rearrangements (dynamics) of the water molecules in the matrix (29).

The thermal evolution of SD_{CO} and SD_{WATER} analyzed in light of MD results (36,37,42) enabled us to infer, in agreement with the water entrapment hypothesis (44), the existence of water molecules at the protein interface involved in HB networks, which anchor the protein to the surrounding matrix (29,30,34). The existence of water molecules at the protein-matrix interface in protein-water-trehalose systems has been recently confirmed by Fayer and co-workers (22).

Analogous FTIR measurements were also performed in samples of MbCO embedded in sucrose-water matrixes (30): in such systems the CO stretching band unequivocally splits into four subbands, thus indicating that the sucrose matrix introduces distortions within the heme pocket, which cause the occurrence of a fourth taxonomic substate. In full agreement, MD simulations of MbCO in trehalose-water and in sucrose-water showed some subtle differences in heme pocket structures (42).

A comparison between the results on trehalose and sucrose (Fig. 1 *b*) samples of similar water content evidenced almost overlapping SD_{WATER} in the whole temperature range investigated. This indicated that, in both the samples, the thermal evolution of the sugar-water matrix is similar. At variance, differences were observed between the two SD_{CO} plots. Such comparison suggested a tighter protein-matrix coupling in trehalose-water than in sucrose-water systems, in full agreement with results of MD simulations (42).

To gain a more general knowledge on the protein-matrix coupling and on the molecular mechanisms at the basis of the trehalose peculiarity, in this work we performed FTIR measurements on MbCO embedded in maltose-water, glucose-water, and raffinose-water matrixes of different water content and analyzed the results together with the ones already reported for trehalose-water and sucrose-water systems (29,30).

Maltose (1,4 α-D-glucopiranosyl-D-glucopyranose, Fig. 1 *c*) was chosen for its similarity to trehalose (1,1′ α, α-D-glucopyranosil-D-glucopyranoside). Indeed, the two disaccharides are identical but for the binding of the second saccharide moiety to the first unit; such binding involves the O1 atom in trehalose, the O4 atom in maltose. Then, at variance from trehalose, maltose is a reducing disaccharide. Glucose (monosaccharide, Fig. 1 *d*) and raffinose (nonreducing trisaccharide, α-galactopyranosyl-(1→6)-α-glucopyranosyl-β-fructofuranoside, Fig. 1 *e*) were chosen to study the effects of the sugar complexity in terms of number of saccharide moieties.

MATERIALS AND METHODS

The shapes of both the CO stretching band and of the water-association band depend on the overall sample composition (sugar, buffer, salts, amount of sodium dithionite, etc.). For this reason we took particular care in preparing samples starting from solutions of identical composition, which differed only in the sugar employed. Furthermore, to compare the outcome of measurements performed in different saccharide matrixes, samples were prepared at equal monosaccharide units molar concentration, rather than at equal sugar molar concentration.

Lyophilized ferric horse myoglobin, maltose, and glucose were purchased from Sigma (St. Louis, MO) and used without further purification. Raffinose from Fluka (Buchs, Switzerland) was used without purification. Ferric myoglobin was dissolved (1×10^{-3} M) in a buffered solution (2×10^{-2} M phosphate buffer, pH 7 in water) containing 4×10^{-1} M of monosaccharide units (i.e., 0.2 M for maltose, 0.4 M for glucose, and 0.133 M for raffinose). The solutions were equilibrated with CO and reduced by anaerobic addition of sodium dithionite (10^{-1} M).

Preparation of maltose and raffinose samples

Maltose and raffinose samples were prepared following the same procedure as for trehalose (29) and sucrose (30). Aliquots (0.1 ml) of the liquid solutions, layered on CaF2 windows, were initially dried for ~8 h under CO atmosphere in a silica gel desiccator at room temperature, then at 353 K for 1 h at atmospheric pressure and afterward ~15 h at 353 K under vacuum. The high temperature treatment, besides drying samples, avoided microcrystals formation (25) as evidenced by the low sample turbidity. Samples were named using a number that indicates the hydration level and a letter which stands for the sugar. Accordingly, $1_{\mathbf{M}}$ is, e.g., the driest maltose sample and $3_{\mathbf{R}}$ the most hydrated raffinose sample; the same terminology was previously used for trehalose and sucrose (30).

To obtain the driest samples studied ($1_{\mathbf{M}}$ and $1_{\mathbf{R}}$), the CaF2 windows on which samples dried at 353 K were layered were put into the sample holder, and transferred into the cryostat, where they were left open to undergo further drying under vacuum at 353 K. Drying ended when the water content, estimated through the area under the band at ~5200 cm^{-1}, resulted, for maltose and raffinose, similar to the one of the driest trehalose and sucrose samples (30). Measurements were then performed in the temperature range 350–20 K. As below reported, it was not possible to lead the glucose sample to analogous dryness.

In Table 1, we report the drying time, within the cryostat at high temperature, needed for leading the various samples to extreme drought.

Samples $2_{\mathbf{M}}$ and $2_{\mathbf{R}}$ were prepared by exposing to room moisture (~3 min at 300 K) the samples dried ~15 h at 353 K under vacuum (see above). Samples were then transferred into the sample holder and confined by putting a Teflon O-ring and a second CaF2 window on top of it to avoid water release during measurements. Samples were then transferred into the cryostat where they were left ~2 h, at room temperature and pressure, before starting measurements. This allowed diffusion of the water absorbed. Measurements were then performed in the temperature range 300–20 K.

To obtain the most humid samples ($3_{\mathbf{M}}$ and $3_{\mathbf{R}}$), the samples dried ~15 h at 353 K under vacuum were overnight equilibrated in the presence of 60% relative humidity at 300 K. The samples were then put into the holder and confined by putting a Teflon O-ring and a second CaF2 window on top of it to avoid water evaporation, and then transferred into the cryostat. Measurements were then performed in the temperature range 300–20 K. After hydration, samples were plastic, not dipping, remaining hard enough to stay in a vertical position within the sample holder.

After the above treatments, all samples remained in an amorphous state as evidenced by the very low turbidity detected by measuring the absorbance at 1900 cm^{-1} at 300 K (25). Measurements of optical absorption and circular dichroism spectroscopy showed that almost full MbCO recovery was

TABLE 1 Drying times, within cryostat, of very dry samples for the different saccharides

Sugar	Drying time (h)
Maltose	1
Glucose	~70
Raffinose	1
Saccharose	3.5
Trehalose	1.5

obtained when redissolving the samples after drying in the desiccator, before heating at 353 K under vacuum. After the high temperature treatment, in the raffinose-coated sample the recovery was almost complete (at the limit of the error, as in trehalose (29)), whereas a lower recovery was obtained (~75%) in maltose, which was even lower than for sucrose-coated samples (~85%) (30). In this respect we note that water uptake by dried samples makes the shape of the CO stretching band to progressively evolve toward a nontreated protein in aqueous solution, thus indicating that damaged protein barely contributes to the signal we analyze.

As already done for trehalose and sucrose samples (30), we performed a qualitative essay (Barfoed essay) on both maltose and raffinose samples after the thermal treatment; this showed that reducing monosaccharides were absent, thus evidencing the lack of temperature-induced sugar degradation.

Preparation of glucose samples

The drying of glucose samples lasted much longer than for the other saccharides (see Table 1). Because of this very low drying rate and of the thermal lability of glucose, the dessication procedure was modified for this sugar. Aliquots (0.1 ml) of MbCO-sugar solution layered on CaF2 windows were initially dried for 10 d under CO atmosphere in silica gel desiccator. Further drying performed as for other sugars at 353 K lead to a ~95–98% protein lost; for this reason we dried the glucose samples under vacuum at 333 K for 12 h. After this procedure, the recovered protein was ~75%.

FTIR measurements on the driest glucose sample started after further drying within the cryostat, where it was left open under vacuum at 333 K. Drying ended when the water content remained constant for a suitable spell of time (>30 min). At the end of this procedure, the water content was still larger than for the driest samples of the other sugars. This made the driest glucose sample more comparable with the dry (No. 2) than with the very dry (No. 1) samples of the other sugars; for this reason, from now on we shall refer to this sample as sample 2_{Ga}.

To ascertain whether this different behavior is due to the different procedure used or to the kind of sugar, we dried a sample of MbCO in trehalose following the same procedure as for sample 2_{Ga}. The water content of such a sample, after drying under vacuum at 333 K for ~10 h, was comparable with that of the below reported sample 1_T. The dry sample (which will be labeled as 2_{Gb}) and the humid, 3_G, sample, are prepared following, after drying at 333K within the desiccator, the same procedure followed for the other sugars. Measurements were then performed in the temperature range 300–20 K.

Water content

In our samples, the high intensity absorption bands of water are covered by signals arising from various components; this lead us to estimate the samples water content by measuring the area (A_C) delimited by the tangent between the two minima to the profile of the band at ~5200 cm^{-1} (at 300 K). In this respect, we note that, in very dry systems, the band splits in two barely resolved subbands.

The reason for choosing this water band, rather than the water-association band, will be discussed in the next section. The used molar absorbance for all samples was 336 L mol^{-1} cm^{-1} (56), under the crude assumption that this quantity is independent on the number of HBs in which water molecules are involved. Since the amounts of myoglobin and of sugar deposited in each sample are always the same, knowing the water content enabled us to get information on the water/sugar and on the water/protein ratios, under the assumption of homogeneous sample thickness, which was estimated using a Palmer micrometer. Obviously, the water/protein ratios refer to the total protein deposited, which may be either carbonilated or noncarbonilated. Furthermore, the ratio is not meant to indicate the number of water molecules directly interacting with each protein but rather the ratio between the whole water to the whole protein present in the sample. The samples water concentration, the water/sugar ratio, and the water/protein ratio of each sample are reported in Table 2.

TABLE 2 Estimated values for the sample water concentration and the water/sugar and water/protein ratios

Sample		Water concentration (M)	≈Water/sugar	≈Water/protein
Trehalose	1_T	0.06	0.3	10
	2_T	0.36	1.8	70
	3_T	5.4	27	1080
Saccharose	1_S	0.06	0.3	10
	2_S	0.99	5.0	200
	3_S	5.7	28.5	1140
Maltose	1_M	0.06	0.3	10
	2_M	1.5	7.5	300
	3_M	3.2	16	640
Glucose	2_{Ga}	0.69	3.4	140
	2_{Gb}	1.9	9.5	380
	3_G	3.3	16.5	660
Raffinose	1_R	0.06	0.3	10
	2_R	0.27	1.4	60
	3_R	2.4	17	680

Water concentration was calculated from the area under the combination band (5200 cm^{-1}) by using a molar absorptivity of 336 L mol^{-1} cm^{-1} and an optical path of 150 μm, estimated using a Palmer micrometer.

All FTIR measurements were performed on a Jasco (Tokyo, Japan) FTIR 410 spectrometer, which has a 2 cm^{-1} resolution. The cryostat and the temperature control used were respectively Optistat CF-V and ITC-503, both from Oxford Instruments (Abingdon, UK).

RESULTS AND DISCUSSION

Water-protein-sugar interactions

According to what we mentioned in the Introduction, two ''subpopulations'' of absorbers contribute to the water-association band; these arise from combinations of the bending mode of water molecules either with intermolecular water-water vibrations or with intermolecular vibrations involving a nonwater HB-forming groups (29,30). Of course, whereas for the latter subpopulation a single water molecule is sufficient for producing a light absorber, this does not hold true for the former. Therefore, the area under the association band linearly depends on water concentration only in two extreme cases: i), in water rich systems, when water-water interaction dominates the band (bulk water); and ii), when only water molecules interacting with nonwater H-bond-forming groups contribute to the band (very dry samples). The last point strictly holds under the assumption that all the subbands of the water-association band share common molar absorbance.

At variance, the water combination band at ~5200 cm^{-1}, which is ascribed to a combination of the water molecule bending and asymmetric stretching, is intramolecular; the area under this band gives, therefore, a less biased estimate of the sample water content than the water-association band (30).

In what follows we shall exploit the different origin of the association and of the combination band to have some hint

on the kind of interactions in which the water molecules in our samples are involved. In Table 3 we report, for all samples, the areas under the profile of the association band (A_A), the areas delimited by the tangent between the two minima to the profile of the water combination band at $\sim$5200 cm^{-1} (A_C), and the ratio $r_A = A_A/A_C$. We also report, as a reference, the same quantities for a sample of crystalline trehalose dihydrate and a sample of pure water (29), i.e., samples in which only one of the above subpopulations contributes to the association band. Since only A_C is proportional to the sample water content, the ratio r_A gives a rough estimate of the relevance of the interactions of water molecules with nonwater H-bond-forming groups. In particular, to larger values of r_A correspond larger fractions of water molecules involved in interactions with nonwater H-bond-forming groups. The high r_A value found for trehalose dihydrate, in which water-water interactions are absent, and the low value found for pure water, where the band only arises from water-water interactions, supports the above suggestion.

As Tables 2 and 3 show all the driest samples, except glucose, have similar water content. However, whereas trehalose and maltose exhibit the same r_A, a slightly lower and a rather larger value is exhibited by sucrose and raffinose, respectively. The behavior of such very dry samples can be rationalized by considering that trehalose, sucrose, and maltose are disaccharides each carrying eight hydroxyl groups. However, in sucrose, intramolecular HBs are present (57) thus leaving an overall lower number of sites available to HB with the surrounding. At variance, in agreement with the large number of coordination water molecules present in its (pentahydrate) crystalline state (58), raffinose directly binds a larger fraction of water molecules than the other sugars (59), as confirmed also by the r_A value for sample 2_R.

Hydrated type 3 samples exhibit low r_A values, thus indicating that water-water interactions mostly dominate the water-association band; as it will be clear when analyzing the thermal behavior of the SD, this does not imply that similar water molecules networks surround the protein.

As Tables 2 and 3 show the water content in the driest glucose sample is one order of magnitude larger than in the driest samples of the other saccharides. Such large water content is paralleled by a rather low r_A value, which approaches the one in pure water and, at variance from the other saccharides, is almost constant at all the hydration levels. This indicates that, in glucose, water-water interactions dominate the water-association band. To understand whether such behavior is peculiar of monosaccharide samples, we analyzed a sample of MbCO embedded in a water-fructose matrix; such a sample behaved as the glucose sample. Based on this observation and on the low r_A value, we inferred that in monosaccharide matrixes interactions among sugar molecules barely led to water extrusion and formation of extended structures, which involve protein sugar and residual water (25). This at variance from dry oligosaccharides, wherein rigid matrixes should originate from the propagation of structures in which water and sugar molecules cross-connect the whole system, thus giving matrixes whose rigidity is modulated by the content of residual water.

TABLE 3 Areas underlying the association band (A_A); areas underlying the combination band (A_C); ratio $r_A = A_A/A_C$

Sugar		A_A	A_C	r_A
Trehalose	1_T	5.5	0.2	27.5
	2_T	7.6	1.2	6.5
	3_T	31.5	18	1.8
Saccharose	1_S	3.9	0.2	19.5
	2_S	9.6	3.3	2.9
	3_S	35.1	19	1.8
Maltose	1_M	5.5	0.2	27.5
	2_M	19	5.3	3.6
	3_M	25.7	10.6	2.4
Glucose	2_{Ga}	4.4	2.3	1.9
	2_{Gb}	14.1	6.4	2.2
	3_G	23.4	11	2.1
Raffinose	1_R	13.6	0.2	68
	2_R	18.2	0.9	20
	3_R	29.3	11.4	2.6
Trehalose dihydrate		21.9	0.3	73
Pure water		313.8	173.6	1.8

Data relative to trehalose dihydrate powders are obtained by reflectance measurements.

CO stretching bands

In Fig. 3 are shown the normalized CO stretching bands at 20 and 300 K, for all the samples studied. We deal with normalized spectra since we are interested in changes of the absorption profile, which reflect heme pocket conformational rearrangements.

As evident, infrared spectra of the bound CO depend on the sugar employed and on the sample water content. As already reported (30), a fourth substate appears in sucrose that cannot be considered as the formerly reported A_2 substate at $\approx$1942 cm^{-1} (47), since its peak frequency is $\sim$1925 cm^{-1}. The same substate appears also in raffinose, although of lower intensity than in sucrose. Since raffinose is a sugar composed by a sucrose molecule that binds a galactose moiety to the O6 of the glucose subunit, we suggest that this substate arises from heme pocket structural modifications induced by sucrose-like units. We attribute the lower intensity of the fourth substate to the lower relative weight of sucrose-like moieties in raffinose than in sucrose samples.

We considered also the possibility that such spectral alteration could arise from the furanoside moiety present in both the sugars: indeed, the lower flexibility of the penta-atomic with respect to the exa-atomic ring (60) might constrain the protein structure in a new substate. CO stretching bands measured in MbCO embedded in fructose-water and ribose-water matrixes did not show the above features (data

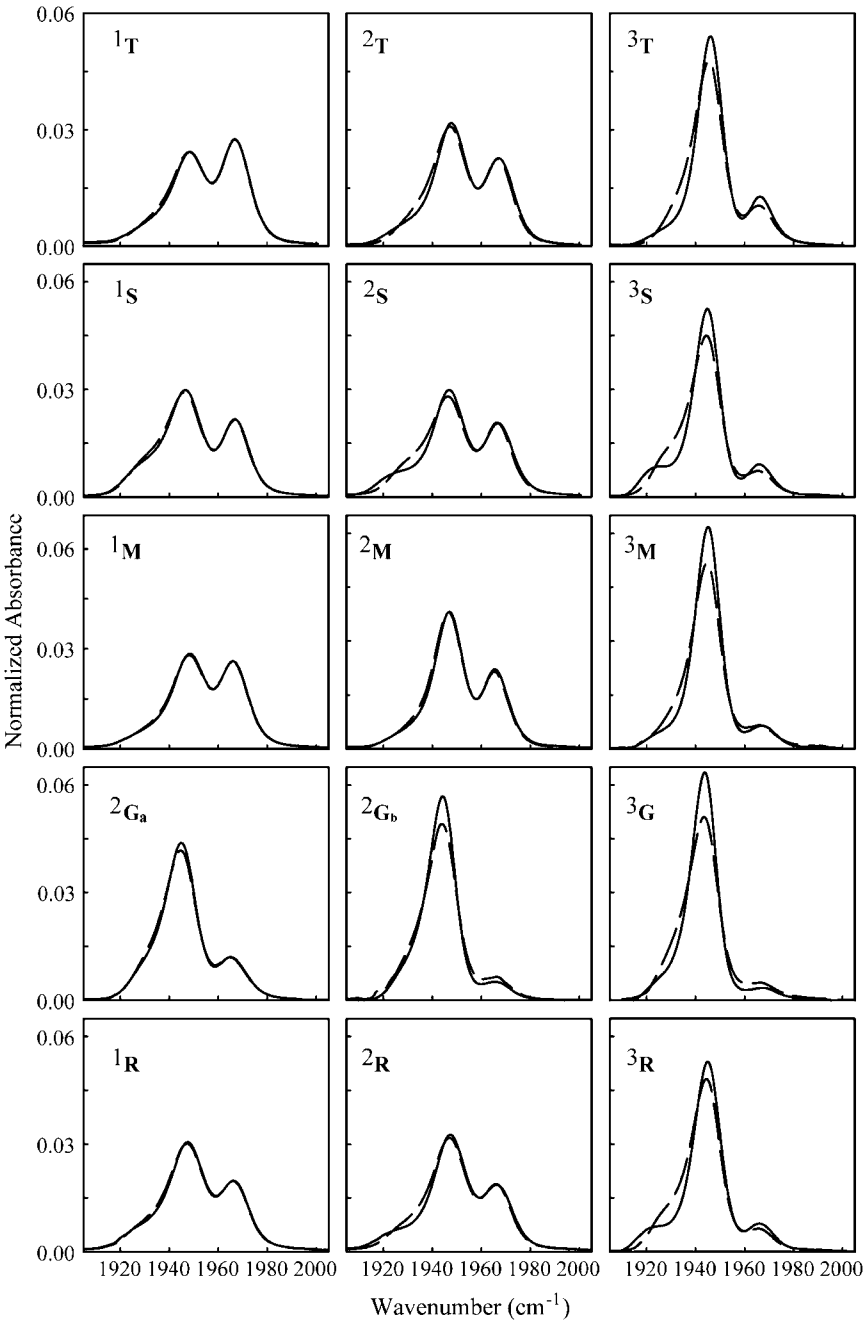

FIGURE 3 Normalized spectra of the CO stretching band at 20 K (*solid lines*) and 300 K (*dashed lines*) for each sample. Results are very well reproducible, within a few percent.

not reported), ruling out the suggestion that interaction of the protein with furanoside moieties could cause the appearance of the fourth substate. Maltose and trehalose samples have very similar CO spectra, differing only for a slightly lower population of the A_0 substate in maltose with respect to trehalose.

At variance from the other sugar systems, the shape of the CO stretching bands exhibits, in all glucose samples, a very low dependence on residual water and looks most like those in humid samples of the other saccharides. In particular, even in sample $2_{\mathbf{Ga}}$ the CO band is more similar to the one in aqueous solution than in the $2_{\mathbf{S}}$ or $2_{\mathbf{M}}$ samples, which still have larger water content than $2_{\mathbf{Ga}}$ sample. This behavior is in line with the observation that hard amorphous matrixes do not form in monosaccharide-containing samples.

Water-association bands

Normalized absorption profiles of the water-association band at 20 and 300 K are shown in Fig. 4. Again, we deal with normalized spectra since we are interested in variations of the band shape, which contain information on structural

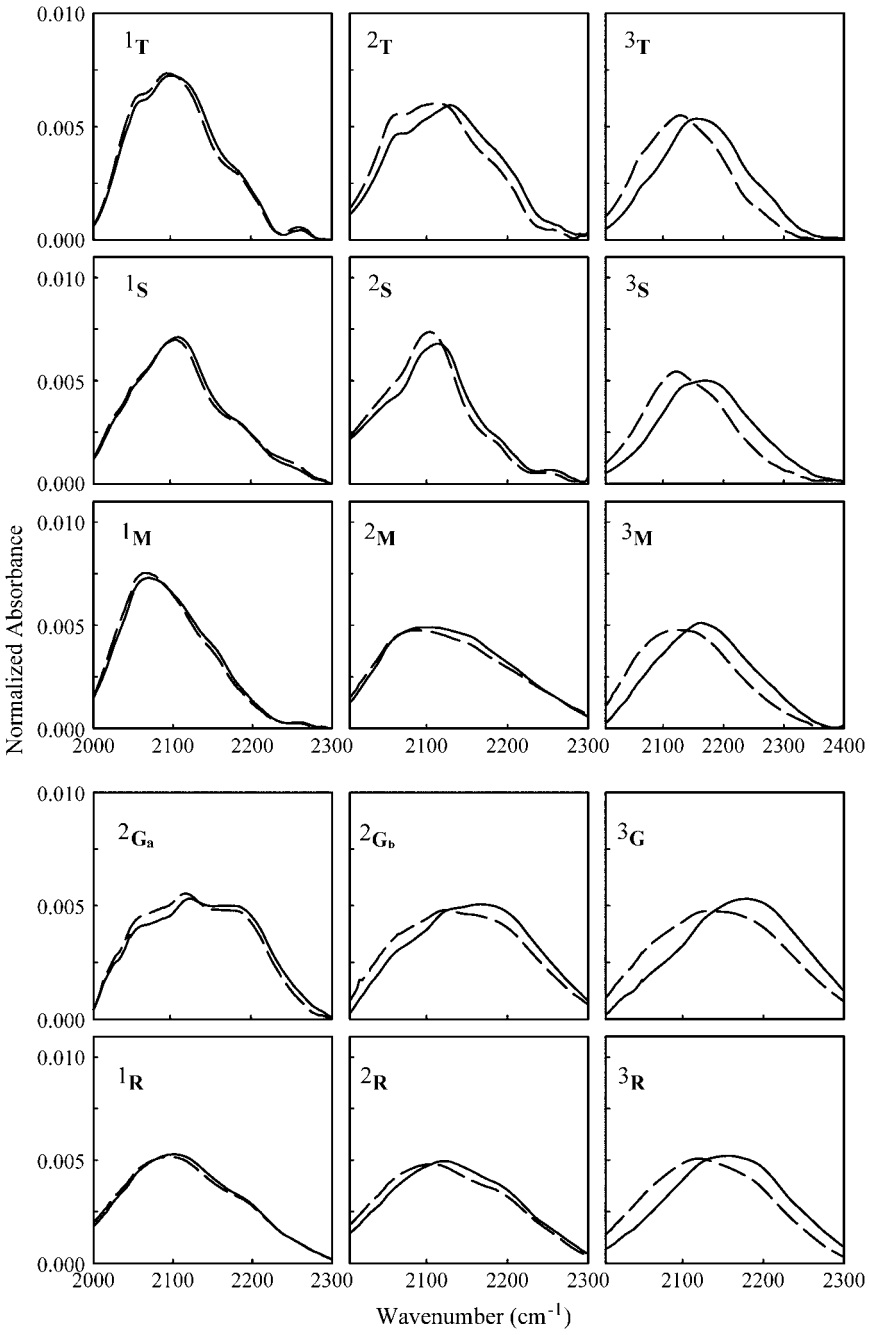

FIGURE 4 Normalized spectra of the water-association band at 20 K (*solid lines*) and 300 K (*dashed lines*) for each sample. Results are very well reproducible, within a few percent.

rearrangements of the water dipoles network, irrespective of the temperature-induced variations of the band oscillator strength.

Each sugar shows a typical shape arising from a different population of the different subbands' components; this is particularly evident in very dry samples. Rather similar profiles are instead evident in humid samples; this is expected since, as also indicated by the r_A values, the water association band in such samples is mostly dominated by water-water interactions. Notwithstanding the large differences in shape among the water-association band in the different samples, a constant set of five subbands fits the bands in all the samples we studied (data not shown).

Spectra distances

Figs. 5–7 show the SD (see Eq. 1) of the water-association bands (SD_{WATER}) and of the CO stretching bands (SD_{CO}), referred to the spectrum at 20 K, for all the sugar analyzed.

As mentioned in the Introduction, the thermal evolution of SD_{CO} is assumed to reflect the overall thermally induced structural changes of the protein, as experienced by the bound CO molecule. Since changes in the conformation of a protein arise from movements between different minima of the energy landscape, it follows that structural changes in the protein are strictly related to the amplitude of nonharmonic,

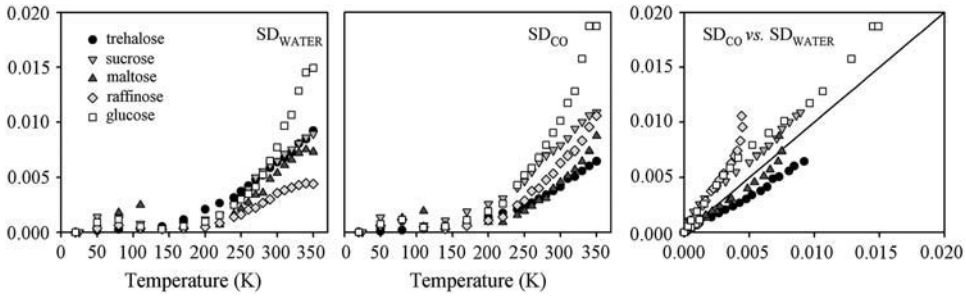

FIGURE 5 (*Left* to *right*) Water-association band spectra distance (SD_{WATER}) referred to the spectrum measured at 20 K versus temperature; CO stretching band spectra distance (SD_{CO}) versus temperature; plot of the SD_{CO} versus the SD_{WATER}. Data refer to the very dry samples. The very good reproducibility of the data points obtained when cycling the temperature indicated that data points are taken under thermal equilibrium (data not shown; see, e.g., Giuffrida et al. (29,30)). Note the scale difference among Figs. 5–7.

atomic mean-square displacements (MSDs). Accordingly, it has been assumed (34) that the temperature dependence of SD_{WATER}, which reflects the thermally induced rearrangements of the water molecules in the matrix (29), parallels the motional freedom of water molecules.

The internal dynamics of a protein is tightly coupled to the dynamics of its hydration shell (61). In particular, it has been suggested (61–63) that water translational motions, which allow complete exchange of protein-bound water molecules by translational displacement, is necessary for large-scale fluctuations involving displacements of the protein surface, as e.g., interconversion among high tier substates and structural relaxations (16,28–30,34). At variance, it appears that exchange of protein-water HBs by water rotational/librational motions (61–63) is not sufficient to permit large-scale internal motions but still allows interconversion among low tiers conformational substates. Therefore one can infer that SD_{CO}, besides giving information on the heme pocket thermal readjustments, also gives indirect information on the mobility of the water molecules at the protein-matrix interface. Then the correlation between SD_{CO} and SD_{WATER}, besides giving information on the protein-matrix coupling, also conveys information on the coupling between water molecules at the protein interface and the distant, bulk water molecules.

In a recent article, Sokolov and co-workers (64) reported on the internal dynamics of tRNA and lysozyme in dry (freeze-dried) samples and in samples of the same biomolecules, which after having been freeze-dried were hydrated in the presence of 98% relative humidity to 0.59 g of D_2O/g tRNA and 0.45 g of D_2O/g protein, respectively. The comparison between the results relative to lysozyme and to tRNA enabled the authors to conclude that in freeze-dried lysozyme nonharmonic internal motions (perhaps related to the methyl groups dynamics) are present; such motions starting from very low temperature and monotonically increasing up to 300 K. At variance, wet protein behave as dry protein only up to ≈200 K: above such temperature, due to the transition of solid-like to liquid-like dynamics of the hydration water, a sharp MSD increase is observed stemming from large-scale motions, which involve displacements of the protein surface. Such behavior parallels the results by Tobias and co-workers (65), who reported the MSDs of methyl protons from MD simulation on hydrated RNase and on dry RNase powders (0.42 and 0.05 g of D_2O per g of protein, respectively (66)).

It has been long ago reported that water molecules bound to protein charged or polar groups exhibit rather large binding energy (67); this makes it extremely difficult to reduce the hydration of a protein below ~0.05 g of H2O/g protein. Therefore, one expects the water content of the dry (freeze dried) lysozyme sample, studied in Caliskan et al. (64), to be comparable to that of the simulated dry RNase powder (65). One can therefore conceive that the observed low tier motions originate from exchange of protein-water HBs via the rotational/librational motions of such water molecules. In what follows, we shall analyze the SDs shown in Figs. 4–6 in light of the data reported in Caliskan et al. (64) and Curtis et al. (65) under the obvious assumption that the thermal behavior of the nonharmonic mean-squared fluctuations

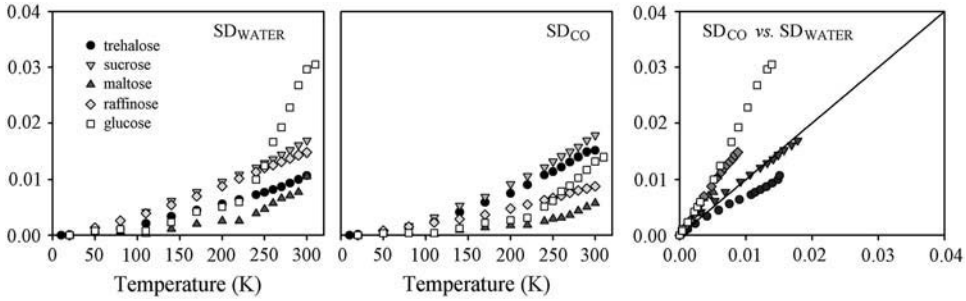

FIGURE 6 As in Fig. 5, for dry samples.

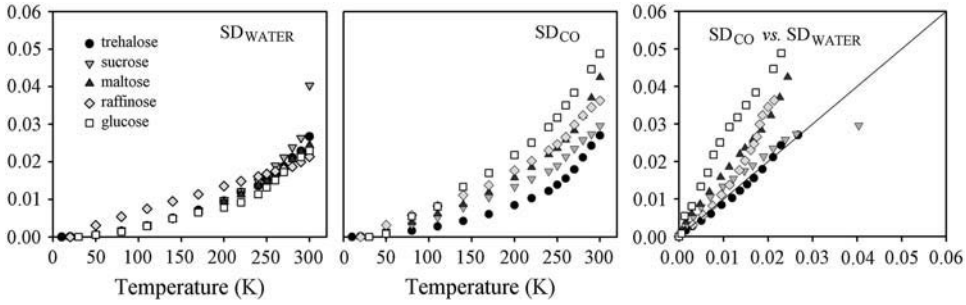

FIGURE 7 As in Fig. 5, for humid samples.

of internal protein motions parallels the thermally induced interconversion among conformational substates.

In very dry samples (Fig. 5) in which residual water molecules are expected to be essentially bonded via four HBs (37), both SD_{CO} and SD_{WATER} are almost vanishing up to ~200 K for all sugars. This indicates lack of structural changes both in the protein and in the matrix and implies that, within our sensitivity, only harmonic atomic motions are present, both in the matrix and in the protein. Above ~200 K a very small increase is evident for both SD_{CO} and SD_{WATER}, stemming from interconversion among very low tiers substates, perhaps related to the onset of rotational/librational motions of the tightly bound water molecules at high temperature. We also report in Fig. 4, for the sake of comparison, the data relative to sample $2_{\mathbf{Ga}}$, which as expected, exhibit larger SD values (see also below).

In dry samples (Fig. 6), both SD_{CO} and SD_{WATER} exhibit a linear behavior, which starts from very low temperature for trehalose, sucrose, and raffinose; the values lying between those measured in the very dry and in the, below reported, humid samples. A sizable change of slope at $T \sim 200$ K is present only for the $2_{\mathbf{Gb}}$ sample, which is consistent with its large water content. The rather monotonic increase of both SD_{WATER} and SD_{CO} for trehalose, sucrose, and raffinose suggests that, in such samples, only low tier processes can take place in the protein interior, coupled to rotational/vibrational fluctuations of water molecules. At variance from very dry systems, such internal processes are present, in dry samples, even at very low temperature, as for dry lysozyme (64) and dry RNase powders (65).

The maltose sample deserves a further comment. Indeed this sample exhibits, among type 2 samples, the lowest SD_{CO} and SD_{WATER}, notwithstanding its larger water content, as compared to other sugars. Furthermore, only for this sugar the SD_{WATER} for dry and extra dry samples overlap in the whole temperature range, whereas slight differences are present, only at high temperature, among the two SD_{CO}. The peculiar behavior of SD_{WATER} for dry maltose samples can be explained on the basis of recent MD simulations results (68), which suggest that maltose-water solutions are inhomogeneous systems in which maltose molecules cluster. Such clustering could be due to the dipole moment of this disaccharide, which is quite larger than for the other saccharides. Dipole moment values calculated from the crystallographic structures of saccharides at the BLYP/6-31G** level are as follows: trehalose, 1.5D; sucrose, 2.5D; maltose, 5.2D; glucose, 1.4D for the β-anomer, 2.5 D for the α-anomer; raffinose, 4.3 D. It is therefore conceivable that the water molecules remain blocked at such clusters to the same extent as in a very dry system. The less constrained water molecules at the protein surface could be responsible for the slight differences between SD_{CO} and SD_{WATER} observed at high temperature.

In the humid sample (Fig. 6), SD_{WATER} for the trehalose, sucrose, maltose, and glucose samples almost overlap in the whole temperature range investigated. Furthermore, they exhibit a rather linear evolution (similar to the one exhibited by dry samples) which starts at ~50 K, followed by a change of slope for $T >$ ~200 K. Such behavior suggests that below 200 K, water molecules are involved in rigid HB networks, which hinder their translational motions only allowing rotational/librational fluctuations. Above ~200 K, due to the release of the HB networks, water molecule translations are allowed over the whole sample, which is reflected in the SD_{WATER} change of slope. At variance from other sugars, in raffinose SD_{WATER} exhibits a linear behavior from cryogenic to room temperature; such a behavior could arise from the large fraction of water molecules directly bound to the sugar (see Table 3 and the relative discussion). This, conceivably, makes the water-sugar interactions to fully regulate the water molecules motional freedom, thus avoiding the formation of an extended HB network governed by water-water interactions, which collapse at ~200 K.

For humid samples, the SD_{CO} plots are rather linear up to ~200 K and change slope above such temperature for all sugars, including raffinose. The low temperature behavior indicates that below ~200 K the hindering of translational motions, evidenced by SD_{WATER}, involves also the water molecules at the protein-matrix interface. Furthermore, the different SD_{CO} plots are not overlapping over the whole temperature range, in line with the different protein-water-sugar structures observed by MD simulation in different sugar systems ((42) and G. Cottone, S. Guiffrida, and L. Cordone, unpublished). One can then infer that water rotational/librational motions at the protein interface are peculiar for each sugar system and produce different protein internal processes, as evidenced by SD_{CO}.

At higher temperature, after the collapse of the HB network (evidenced by SD_{WATER} for all sugars but raffinose)

translational displacement of protein-bound water also enables large-scale substates interconversion and protein structural relaxations. These motions, which are reflected in the deviation of SD_{CO} from the linear behavior, involve displacements of the protein surfaces (16,29,30,34) and have been suggested to be driven by fluctuations of the dielectric constant of the medium (69), which implies water molecules translational freedom. Large-scale substates interconversion is already evidenced in the raw CO spectra of humid samples, shown in Fig. 3.

The peculiar behavior of raffinose, for which the change of slope is present in SD_{CO} and absent in SD_{WATER}, can be rationalized by considering that the onset of large-scale heme pocket fluctuations (reflected in SD_{CO}) is indicative of translational motions at the protein interface, which, in view of the behavior of SD_{WATER}, does not extend to the whole bulk matrix (see the above discussion on dry samples). Since, in humid samples, the water molecules in the neighbor of the protein are only a fraction of the overall water molecules, their relative weight on SD_{WATER} may be, plausibly, covered by signal arising from water molecules far from the protein surface. Such an effect is expected to play a relevant role only in raffinose where SD_{WATER} seems to be mostly governed by water-sugar interactions.

The different protein-matrix coupling is better evidenced in the correlation plots in Figs. 5–7. In particular, in the humid trehalose sample, the protein is well matched to the whole matrix. Indeed, in this sample the slope of the correlation plot is unitary over the whole temperature range investigated; this suggests a long-range correlation between the water at the protein interface and the bulk water, which propagates over the whole sample (29). In this respect, we point out that the correlation plot gives information both on the protein-matrix coupling and on the coupling between the water at the protein interface and in the distant (bulk) water. We note that the correlation plots for glucose shows larger slopes with respect to other sugars, also in the driest sample; one can, therefore, speculate the poor preservation properties of glucose to arise from the softness of the matrix and the scarce protein-matrix coupling.

Several studies devoted to the dependence of protein internal dynamics on hydration in the absence of sugar (67,70–74) evidenced that many proteins need 100–500 water molecules (67,70) to restore their normal dynamics and function. In this respect we note that our measurements do not enable us to infer the number of water molecules interacting with each proteins, within the saccharide matrixes (see Table 2 and relative discussion). Further, we stress that the same mechanisms of protein-water interactions as in the absence of sugar cannot be invoked to explain our data in sugar matrixes. Rather, our dry systems are to be compared to the protein/fixed-solvent system studied by Vitkup et al. by MD simulations (75), in which the protein fluctuations were found smaller than those in the room temperature solvent, whereas the local motions occurring without distortion of the protein surface were still present. Moreover, MD simulations performed on MbCO-trehalose-water systems (37) at 89% sugar/[sugar + water] w/w and 50% sugar/[sugar + water] w/w (which respectively correspond to 2 and 20 water molecules/sugar molecule) showed that the protein dynamics is sizably hindered, in the hundreds of picoseconds timescale, in the 89% w/w system (in which ~90 water molecules and ~80 sugar hydroxyl groups are hydrogen bonded to the protein), whereas it is not hindered in the softer 50% w/w system (where ~270 water molecules and ~30 hydroxyl groups bound the protein).

CONCLUSIONS

FTIR experiments have been performed on samples of MbCO embedded in matrixes of different sugars and content of residual water. A suitable analysis based on the thermal behavior of the SD relative to both the stretching band of the ligand CO molecule (SD_{CO}) and the water-association band (SD_{WATER}) (29,30,34) showed that the thermal evolution of sugar-water matrix barely depends on the particular saccharide, whereas the sample water content regulates the amplitude of protein internal motions in a way which is peculiar for each sugar. General features that can be inferred from our FTIR data are:

i. In very dry samples having a water/sugar mole ratio of ~0.3, only very low scale motions are allowed, even at room temperature. In this respect, we point out that room temperature flash photolysis measurements (34) in a very dry trehalose sample pointed out the lack of diffusion of the flashed off CO even in the distal heme pocket side.
ii. In samples of low water/sugar mole ratio (in the range ~2−10, dry samples), only low scale motions as the ones involving rotations and librations of water molecules (in the matrix) and interconversion among low tier protein conformational substates, take place even at room temperature. In full agreement, flash photolysis measurements (28,34), performed at room temperature in trehalose samples of similar water content, showed that the recombination of CO molecules takes place in a nonrelaxing protein in which large-scale interconversions are hindered. Furthermore, in such samples the HB network, which couples the protein surface to the surrounding matrix, can be temporarily destroyed by continuous illumination (light-induced relaxation) (35).
iii. In samples having a large water/sugar mole ratio (in the range ~16−28), large-scale motions, as the ones involving protein relaxation and interconversion among taxonomic A substates, take place at room temperature; in such samples water molecules translations at the protein interface are allowed at high temperature. In full agreement, previously reported flash photolysis measurements (28,34), performed at room temperature, had shown that in humid MbCO-trehalose samples the

flashed off CO molecule can diffuse within the heme pocket and that the protein can relax. Furthermore, in humid samples, continuous illumination has no effect on the (soft) HB network, which couples the protein to the surroundings (35).

In previous works (30,42), we suggested that the better efficiency as bioprotectant of trehalose with respect to sucrose could be ascribed to the tighter protein-matrix coupling in trehalose with respect to sucrose, since the appearance of damages on biological structures will more involve structural variations of the surrounding matrix. The results in the study presented here enable us to extend this suggestion also to other sugars and enable us to better rationalize why carbohydrates having most similar hydrogen-bonding capability exhibit different efficiency in preserving biomaterials. Furthermore, the protein-matrix coupling is in line with the lack of ''phase separation'' between protein and external sugar matrix in trehalose with respect to lactose, found in lysozyme-sugar systems (76); we suggest that this effect arises from a mismatch between the protein and the sugar-water structures at the protein interface. A similar effect has recently been observed for the reaction center complex purified from *Rhodobacter sphaeroides*, which can be embedded in solid water-trehalose matrixes (31–33), while it undergoes phase separation in sucrose-water systems (Venturoli and coworkers, unpublished.

We believe that the sizable dependence on sample composition of the structural (and dynamic) coupling between a protein and its surrounding should play a most relevant role in pattern recognitions among biomolecules in crowded living system. In this respect, we note that, as shown in the correlation plot (SD_{CO} versus SD_{WATER}) in the humid trehalose sample, the thermal evolution of the water HB network parallels the thermal evolution of the heme pocket; this suggests the coupling to be long-range under favorable conditions of the protein surroundings. Accordingly, we expect that suitable dynamic-structure matching between the ''hydration clouds'' of approaching molecules will lead to successful come together.

This work was supported by MIUR (grant PRIN 2005, Proprietà Dinamiche Strutturali e Funzionali di Proteine in Sistemi Non-Liquidi Contenenti Acqua Residua: Accoppiamento con la Matrice Esterna) and local fundings (ex 60%).

REFERENCES

1. Crowe, J. H., and L. M. Crowe. 1984. Preservation of membranes in anhydrobiotic organisms: the role of trehalose. *Science.* 223:701–703.
2. Bianchi, G., A. Gamba, C. Murellie, F. Salamini, and D. Bartels. 1991. Novel carbohydrate metabolism in the resurrection plant. *Craterostigma plantagineum. Plant J.* 1:355–359.
3. Uritani, M., M. Takai, and K. Yoshinaga. 1995. Protective effect of disaccharides on restriction endonucleases during drying under vacuum. *J. Biochem. (Tokyo).* 117:774–779.
4. Panek, A. D. 1995. Trehalose metabolism—new horizons in technological applications. *Braz. J. Med. Biol. Res.* 28:169–181.
5. Crowe, L. M. 2002. Lesson from nature: a role of sugars in anhydrobiosis. *Comp. Biochem. Physiol. A.* 132:505–513.
6. Crowe, J. H., L. M. Crowe, and S. A. Jackson. 1983. Preservation of structural and functional activity in lyophilized sarcoplasmic reticulum. *Arch. Biochem. Biophys.* 220:615–617.
7. Crowe, L. M., and J. H. Crowe. 1995. Freeze-dried liposomes. *In* Liposomes, New Systems and New Trends in Their Applications. F. Puisieux, P. Covreur, L. Delattre, and J. P. Devissaguet, editors. Editions de Santè, Paris. 237–272.
8. Chiantia, S., L. I. Giannola, and L. Cordone. 2005. Lipid phase transition in saccharide-coated cholate-containing liposomes: coupling to the surrounding matrix. *Langmuir.* 21:4108–4116.
9. Lambruschini, C., A. Relini, A. Ridi, L. Cordone, and A. Gliozzi. 2000. Trehalose interacts with phospholipid polar heads in langmuir monolayers. *Langmuir.* 16:5467–5470.
10. Hagen, S. J., J. Hofrichter, and W. A. Eaton. 1995. Protein reaction kinetics in a room temperature glass. *Science.* 269:959–962.
11. Hagen, S. J., J. Hofrichter, and W. A. Eaton. 1996. Geminate rebinding and conformational dynamics of myoglobin embedded in a glass at room temperature. *J. Phys. Chem.* 100:12008–12021.
12. Gottfried, D. S., E. S. Peterson, A. G. Sheikh, J. Wang, M. Yang, and J. M. Friedman. 1996. Evidence for damped hemoglobin dynamics in a room temperature glass. *J. Phys. Chem.* 100:12034–12042.
13. Sastry, G. M., and N. Agmon. 1997. Trehalose prevents myoglobin collapse and preserves its internal mobility. *Biochemistry.* 36:7097–7108.
14. Kleinert, T., W. Doster, H. Leyser, W. Petry, V. Schwarz, and M. Settles. 1998. Solvent composition and viscosity effects on the kinetics of CO binding to horse myoglobin. *Biochemistry.* 37:717–733.
15. Lichtenegger, H., W. Doster, T. Kleinert, A. Birk, B. Sepiol, and G. Vogl. 1999. Heme-solvent coupling: a Mössbauer study of myoglobin in sucrose. *Biophys. J.* 76:414–422.
16. Rector, D., J. Jiang, M. A. Berg, and M. D. Fayer. 2001. Effects of solvent viscosity on protein dynamics: infrared vibrational echo experiments and theory. *J. Phys. Chem. B.* 105:1081–1092.
17. Schlichter, J., J. Friedrich, L. Herenyi, and J. Fidy. 2001. Trehalose effect on low temperature protein dynamics: fluctuation and relaxation phenomena. *Biophys. J.* 80:2011–2017.
18. Dantsker, D., U. Samuni, A. J. Friedman, M. Yang, A. Ray, and J. M. Friedman. 2002. Geminate rebinding in trehalose-glass embedded myoglobins reveals residue-specific control of intramolecular trajectories. *J. Mol. Biol.* 315:239–251.
19. Ponkratov, V. V., J. Friedrich, and J. M. Vanderkooi. 2002. Solvent effect on conformational dynamics of proteins: cytochrome *c* in a dried trehalose film. *J. Chem. Phys.* 117:4594–4601.
20. Mei, E., J. Tang, J. M. Vanderkooi, and J. M. Hochstrasser. 2003. Motions of single molecules and proteins in trehalose glass. *J. Am. Chem. Soc.* 125:2730–2735.
21. Caliskan, G., D. Mechtani, J. H. Roh, A. Kisliuk, A. P. Sokolov, S. Azzam, M. T. Cicerone, S. Lin-Gibson, and I. Peral. 2004. Protein and solvent dynamics: how strongly are they coupled? *J. Chem. Phys.* 121:1978–1983.
22. Massari, A. M., I. J. Finkestein, B. L. McClain, A. Goj, X. Wen, K. L. Bren, R. F. Loring, and M. D. Fayer. 2005. The influence of aqueous versus glassy solvents on protein dynamics. Vibrational echo experiments and molecular dynamics simulations. *J. Am. Chem. Soc.* 127: 14279–14289.
23. Cordone, L., P. Galajda, E. Vitrano, A. Gassmann, A. Ostermann, and F. Parak. 1998. A reduction of protein specific motions in co-ligated myoglobin embedded in a trehalose glass. *Eur. Biophys. J.* 27:173–176.
24. Cordone, L., M. Ferrand, E. Vitrano, and G. Zaccai. 1999. Harmonic behavior of trehalose-coated carbon-monoxy-myoglobin at high temperature. *Biophys. J.* 76:1043–1047.
25. Librizzi, F., E. Vitrano, and L. Cordone. 1999. Dehydration and crystallization of trehalose and sucrose glasses containing carbon-monoxy-myoglobin. *Biophys. J.* 76:2727–2734.

26. Librizzi, F., E. Vitrano, and L. Cordone. 1999. Inhibition of A substates interconversion in trehalose coated carbonmonoxy-myoglobin. *In* Biological Physics. H. Frauenfelder, G. Hummer, and R. Garcia, editors. AIP American Institute of Physics, Melville, NY. 132–138.
27. Librizzi, F., A. Paciaroni, C. Pfister, E. Vitrano, G. Zaccai, and L. Cordone. 2001. Dynamical properties of carbonmonoxy-myoglobin embedded in trehalose matrixes of different water content studied by FTIR and elastic neutron scattering. *In* Proceedings of ILL Millennium Symposium and European User Meeting, Institute Laue-Langevin, Grenoble. 58–59.
28. Librizzi, F., C. Viappiani, S. Abbruzzetti, and L. Cordone. 2002. Residual water modulates the dynamics of the protein and of the external matrix in ''trehalose coated'' MbCO: an infrared and flash photolysis study. *J. Chem. Phys.* 116:1193–1200.
29. Giuffrida, S., G. Cottone, F. Librizzi, and L. Cordone. 2003. Coupling between the thermal evolution of the heme pocket and the external matrix structure in trehalose coated carboxymyoglobin. *J. Phys. Chem. B.* 107:13211–13217.
30. Giuffrida, S., G. Cottone, and L. Cordone. 2004. Structure-dynamics coupling between protein and external matrix in sucrose coated and in trehalose coated MbCO: an FTIR study. *J. Phys. Chem. B.* 108: 15415–15421.
31. Palazzo, G., A. Mallardi, A. Hochkoeppler, L. Cordone, and G. Venturoli. 2002. Electron transfer in photosynthetic reaction center embedded in trehalose glasses: trapping of conformational substates at room temperature. *Biophys. J.* 82:558–568.
32. Francia, F., G. Palazzo, A. Mallardi, L. Cordone, and G. Venturoli. 2004. Probing light-induced conformational transitions in bacterial photosynthetic reaction centers embedded in trehalose amorphous matrixes. *Biochim. Biophys. Acta.* 1658:50–57.
33. Francia, F., G. Palazzo, A. Mallardi, L. Cordone, and G. Venturoli. 2003. Residual water modulates Q_A^- to Q_B electron transfer in bacterial reaction centers embedded in trehalose amorphous matrixes. *Biophys. J.* 85:2760–2775.
34. Cordone, L., G. Cottone, S. Giuffrida, G. Palazzo, G. Venturoli, and C. Viappiani. 2005. Internal dynamics and protein-matrix coupling in trehalose coated proteins. *Biochim. Biophys. Acta.* 1749: 252–281.
35. Abbruzzetti, S., S. Giuffrida, S. Sottini, C. Viappiani, and L. Cordone. 2005. Light-induced protein-matrix uncoupling and protein relaxation in dry samples of trehalose-coated MbCo at room temperature. *Cell Biochem. Biophys.* 43:431–438.
36. Cottone, G., L. Cordone, and G. Ciccotti. 2001. Molecular dynamics simulation of carboxy-myoglobin embedded in a trehalose-water matrix. *Biophys. J.* 80:931–938.
37. Cottone, G., G. Ciccotti, and L. Cordone. 2002. Protein-trehalose-water structures in trehalose coated carboxy-myoglobin. *J. Chem. Phys.* 117: 9862–9866.
38. Lins, R. D., C. S. Pereira, and P. H. Hunenberger. 2004. Trehalose-protein interaction in aqueous solution. *Proteins.* 55:177–186.
39. Sum, A. K., R. Faller, and J. J. de Pablo. 2003. Molecular simulation study of phospholipid bilayers and insights of the interactions with disaccharides. *Biophys. J.* 85:2830–2844.
40. Pereira, C. S., R. D. Lins, I. Chandrasekhar, L. C. G. Freitas, and P. H. Hunenberger. 2004. Interaction of the disaccharide trehalose with a phospholipid bilayer: a molecular dynamics study. *Biophys. J.* 86: 2273–2285.
41. Villarreal, M. A., S. B. Dyaz, E. A. Disalvo, and G. G. Montich. 2004. Molecular dynamics simulation study of the interaction of trehalose with lipid membranes. *Langmuir.* 20:7844–7851.
42. Cottone, G., S. Giuffrida, G. Ciccotti, and L. Cordone. 2005. Molecular dynamics simulation of sucrose- and trehalose-coated carboxy-myoglobin. *Proteins.* 59:291–302.
43. Carpenter, J. F., and J. H. Crowe. 1989. An infrared spectroscopic study of the interaction of carbohydrates with dried proteins. *Biochemistry.* 28:3916–3922.
44. Belton, P. S., and A. M. Gil. 1994. IR and Raman spectroscopic studies of the interaction of trehalose with hen egg white lysozyme. *Biopolymers.* 34:957–961.
45. Sampedro, J. G., and S. Uribe. 2004. Trehalose-enzyme interactions result in structure stabilization and activity inhibition. *Mol. Cell. Biochem.* 256:319–327.
46. Green, J., and C. A. Angell. 1989. Phase relations and vitrification in saccharide-water solutions and the trehalose anomaly. *J. Phys. Chem.* 93:2880–2882.
47. Frauenfelder, H., F. Parak, and R. D. Young. 1988. Conformational substates in proteins. *Annu. Rev. Biophys. Chem.* 17:451–479.
48. Vojtechovsky, J., K. Chu, J. Berendzen, R. M. Sweet, and I. Schlichting. 1999. Crystal structures of myoglobin-ligand complexes at near-atomic resolution. *Biophys. J.* 77:2153–2174.
49. Ansari, A., J. Berendzen, D. Braunstein, B. R. Cowen, H. Frauenfelder, M. K. Hong, I. E. T. Iben, J. B. Johnson, P. Ormos, T. B. Sauke, R. Scholl, A. Schulte, P. J. Steinbach, J. Vittitow, and R. D. Young. 1987. Rebinding and relaxation in the myoglobin pocket. *Biophys. Chem.* 26:337–355.
50. Ansari, A., C. M. Jones, E. R. Henry, J. Hofrichter, and W. Eaton. 1992. The role of solvent viscosity in the dynamics of protein conformational changes. *Science.* 256:1796–1798.
51. Makinen, M. W., R. A. Houtchens, and W. S. Caughey. 1979. Structure of carboxymyoglobin in crystals and in solutions. *Proc. Natl. Acad. Sci. USA.* 76:6042–6046.
52. Beece, D., L. Eisenstein, H. Frauenfelder, D. Good, M. C. Marden, L. Reinisch, A. H. Reynolds, L. B. Sorensen, and K. T. Yue. 1980. Solvent viscosity and protein dynamics. *Biochemistry.* 19: 5147–5157.
53. Frauenfelder, H., N. A. Alberding, A. Ansari, D. Braunstein, B. R. Cowen, M. K. Hong, I. E. T. Iben, J. B. Johnson, S. Luck, M. C. Marden, J. R. Mourant, P. Ormos, L. Reinisch, R. Scholl, A. Schulte, E. Shyamsunder, L. B. Soremen, P. J. Steinbach, A. Xie, R. D. Young, and K. T. Yue. 1990. Proteins and pressure. *J. Phys. Chem.* 94:1024–1037.
54. Eisenberg, D., and W. Kauzmann. 1969. The Structure and Properties of Water. Oxford University Press, London.
55. Kaposi, A. D., J. M. Vanderkooi, W. W. Wright, J. Fidy, and S. S. Stavrov. 2001. Influence of static and dynamic disorder on the visible and infrared absorption spectra of carbonmonoxy horseradish peroxidase. *Biophys. J.* 81:3472–3482.
56. Dickens, B., and S. H. Dickens. 1999. Estimation of concentration and bonding environment of water dissolved in common solvents using near infrared absorptivity. *J. Res. Natl. Inst. Stand. Technol.* 104: 173–183.
57. Ekdawi-Sever, N. C., P. B. Conrad, and J. J. de Pablo. 2001. Molecular simulation of sucrose solutions near the glass transition temperature. *J. Phys. Chem. A.* 105:734–742.
58. Berman, H. M. 1970. The crystal structure of a trisaccharide, raffinose pentahydrate. *Acta Crystallogr.* 26:290–299.
59. Gaffney, S. H., E. Haslam, T. H. Lilley, and T. R. J. Ward. 1988. Homotactic and heterotactic interactions in aqueous-solutions containing some saccharides experimental results and an empirical relationship between saccharide solvation and solute interactions. *J. Chem. Soc. Faraday Trans.* 84:2545–2552.
60. Rao, V. S. R., P. K. Qasba, P. V. Balaji, and R. Chandrasekaran. 1998. Conformation of Carbohydrates. Harwood Academic Publishers, Newark, NJ.
61. Doster, W., A. Bacheitner, R. Dunau, M. Hiebl, and E. Luscher. 1986. Thermal properties of water in myoglobin crystals and solutions at subzero temperatures. *Biophys. J.* 50:213–219.
62. Tarek, M., and D. J. Tobias. 2000. The dynamics of protein hydration water: a quantitative comparison of molecular dynamics simulations and neutron-scattering experiments. *Biophys. J.* 79:3244–3257.
63. Tarek, M., and D. J. Tobias. 2002. Role of protein-water hydrogen bond dynamics in the protein dynamical transition. *Phys. Rev. Lett.* 88:8101–8104.

64. Caliskan, G., R. M. Briber, D. Thirumalai, V. Garcia-Sakai, S. A. Woodson, and A. P. J. Sokolov. 2006. Dynamic transition in tRNA is solvent induced. *J. Am. Chem. Soc.* 128:32–33.

65. Curtis, J. E., M. Tarek, and D. J. J. Tobias. 2004. Methyl group dynamics as a probe of the protein dynamical transition. *J. Am. Chem. Soc.* 126:15928–15929.

66. Tarek, M., and D. J. J. Tobias. 1999. Environmental dependence of the dynamics of protein hydration water. *J. Am. Chem. Soc.* 121:9740–9741.

67. Rupley, J. A., E. Gratton, and G. Careri. 1983. Water and globular proteins. *Trends Biochem. Sci.* 8:18–22.

68. Lerbret, A., P. Bordat, F. Affouard, M. Descamps, and F. Migliardo. 2005. How homogeneous are the trehalose, maltose, and sucrose water solutions? An insight from molecular dynamics simulations. *J. Phys. Chem.* 109:11046–11057.

69. Fenimore, P. W., H. Frauenfelder, B. H. McMahon, and F. G. Parak. 2002. Slaving: solvent fluctuations dominate protein dynamics and functions. *Proc. Natl. Acad. Sci. USA.* 99:16047–16051.

70. Doster, W., S. Cusak, and W. Petry. 1989. Dynamical transition of myoglobin revealed by inelastic neutron scattering. *Nature.* 337:754–756.

71. Doster, W. 1999. The dynamical transition in proteins: the role of hydrogen bonds. *In* Hydration Processes in Biology. M. C. Bellissent-Funel, editor. IOS Press, Amsterdam, The Netherlands. 177–191.

72. Parak, F., M. Fisher, E. Graffweg, and H. Formanek. 1986. Distributions and fluctuations of protein structures investigated by x-ray analysis and Mossbauer spectroscopy. *In* Structure and Dynamics of Nucleic Acids, Proteins and Membranes. E. Clementi and S. Chin, editors. Plenum Press, New York. 139–148.

73. Goldanskii, V. I., and Y. F. Krupyanskii. 1989. Protein and protein-bound water dynamics studied by Raileigh scattering of Mossabuer radiation (RSMR). *Q. Rev. Biophys.* 22:39–92.

74. Steinbach, P. J., R. J. Loncharich, and B. R. Brooks. 1991. The effects of environment and hydration on protein dynamics: a simulation study of myoglobin. *Chem. Phys.* 158:383–394.

75. Vitkup, D., D. Ringe, G. A. Petsko, and M. Karplus. 2000. Solvent mobility and the protein 'glass' transition. *Nat. Struct. Biol.* 7:34–38.

76. Lam, Y. H., R. Bustami, T. Phan, H. K. Chan, and F. Separovic. 2002. A solid-state NMR study of protein mobility in lyophilized protein-sugar powders. *J. Pharm. Sci.* 91:943–951.